International Conference on Applied Energy 2020
Dec. 1 - Dec. 10, 2020, Bangkok / Virtual
Paper ID: 0469

Numerical investigation on adsorption chamber with internal heat exchanger for temperatue swing CO_2 adsorption

Lijin Chen[1,2], Shuai Deng[1,2*], Ruikai Zhao[1,2], Li Zhao[1]

1 Key Laboratory of Efficient Utilization of Low and Medium Grade Energy (Tianjin University), Ministry of Education of China, Tianjin 300350, China

2 International Cooperation Research Center of Carbon Capture in Ultra-low Energy-Consumption, Tianjin 300350, China

ABSTRACT

In order to enhance heat and mass exchange, the internal heat exchanger is introduced into the adsorption chamber based on the temperature swing adsorption (TSA) process. Heating is carried out by condensing steam, and cooling by water circulation. The influence of the number of internal heat exchangers, inlet speed and porosity on the CO_2 purity, recovery rate, energy consumption and COP_{CO_2} are discussed numerically to improve the energy efficiency performance of TSA process. The results show that under the same operating conditions, the CO_2 purity, recovery rate and COP_{CO_2} of the three-tube heat exchanger in adsorption chamber are higher than that of the one-tube heat exchanger, with lower energy consumption of three-tube heat exchanger. The temperature distribution of the adsorption chamber is greatly influenced by the inlet speed and porosity. By increasing inlet speed or porosity, the CO_2 purity, recovery rate and COP_{CO_2} can be improved and energy consumption can be reduced. The obtained simulation results can provide further guidance for engineering design.

Keywords: Temperature swing adsorption, adsorption chamber, heat exchanger, numerical simulation and optimization

NONMENCLATURE

Abbreviations	
ε	the chamber porosity
ρ	density, kg/m^3
δ	chamber wall thickness, m
A	the heat transfer area, m^2
C	the component concentration, mol/m^3
$C_{p,w}$	the specific heat capacity of wall material, J/kg K
$C_{p,s}$	the specific heat capacity of adsorbent, J/kg K
D	diameter, m
F	the molar flow rate, mol/s
ΔH	the heat of adsorption, J/mol
K_{eq}	the isotherm adsorption constant, 1/Pa
K_0	the Toth adsorption constant, 1/Pa
Q_F	the volumetric flow rate, m^3 /s
q^*	the equilibrium adsorption uptake, mol/kg
q_m	the maximum adsorption uptake, mol/kg
R	universal gas constant, J/mol K

1. INTRODUCTION

In September 2020, China promised at the United Nations General Assembly to strive to achieve carbon neutrality by 2060[1]. Since CO_2 is considered the main promoter for climate change, carbon capture (CC) is an essential solution to keep using fossil fuels while minimizing the emissions of CO_2 into the atmosphere, and thereby mitigating global climate change[2]. CO_2 capture technology, especially temperature swing adsorption (TSA) is attractive due to the non-volatility of solid sorbents, the potentially low energy consumption[3] due to the moderate heat of adsorption (between 25 kJ/mol and 50 kJ/mol[4-5]) and the moderate desorption temperature, which might offer attractive heat integration opportunities using low-grade heat sources[6].

Most of TSA cycles use steam desorption or direct hot gas circulation heating for the desorption[7]. In the former situation, the adsorbent must be dried out after the steam circulation and, in addition, a supplementary process for the separation of the adsorbate from the

Selection and peer-review under responsibility of the scientific committee of the 12th Int. Conf. on Applied Energy (ICAE2020).

steam or water must be operated. In the latter case, the desorbed phase is diluted so that the recovery of the adsorbate remains limited. For these reasons, various processes avoiding a direct heating have been developed, among which electrothermal desorption (Joule effect heating)[8-9] and microwave heating[10] uses thermoelectric devices[11]. Therefore, to solve these challenges, the present work aim at the combination of adsorption chamber and internal heat exchanger.

In this paper, a three-dimensional heat exchanger in adsorption chamber model is established and verified. The effects of inlet speed and porosity on the heat and mass transfer in the one and three tube heat exchangers in the adsorption chambers were simulated and compared. This study provides some engineering guidance for the industrial development of carbon capture technology.

2. MODELING DESCRIPTION

2.1 Adsorption chamber

The combination of adsorption chamber and heat exchanger can adjust the chamber temperature and enhance heat and mass transfer. However, due to different types of heat exchangers and the structure and number of internal heat exchangers in the adsorption chamber, the guidance of simulation results for practical engineering remains to be discussed.

The three-dimensional model of the adsorption chambers of single and three tube heat exchangers are shown in Fig. 1. FLUENT ANSYS software was used to load mass, momentum and energy source terms and conduct numerical simulation calculation[12].

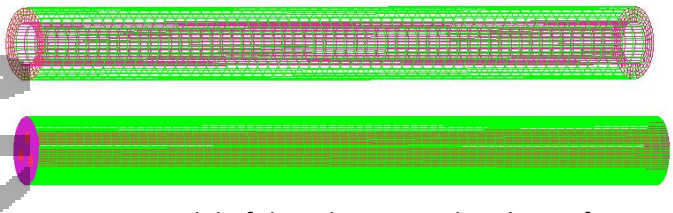

Fig. 1. 3D model of the adsorption chambers of one and three tube heat exchangers

The mass equation can be expressed as follows.

$$\frac{\partial(\varepsilon\rho)}{\partial t}+div(\rho\vec{v})=-(1-\varepsilon)\rho_p\sum_i M_i\frac{\partial q_i}{\partial t} \tag{1}$$

The formula $\frac{\partial q}{\partial t}$ requires the joint solution of the adsorption equilibrium model and adsorption kinetics model. In this paper, the Toth model is exploited for gases equilibrium adsorption.

$$q_i^*=\frac{q_{m,i}K_{eq,i}p_i}{\left(1+(K_ip_i)^{n_i}\right)^{\left(\frac{1}{n_i}\right)}} \tag{2}$$

$$K_{eq,i}=k_0e^{-\left(\frac{\Delta H}{RT}\right)} \tag{3}$$

The adsorption kinetics adopted linear driving force (LDF) model.

$$\frac{\partial q_i}{\partial t}=k_{L,i}\left(q_i^*-q_i\right) \tag{4}$$

Farooq and Ruthven[13] proposed that the calculation of mass transfer coefficient needs to take the membrane resistance, macro-porous resistance and microporous resistance into account. The formula for calculating the mass transfer coefficient is as follows.

$$\frac{1}{k_{L,i}}=\frac{r_p}{3k_{f,i}}+\frac{r^2{}_p}{15\varepsilon_pk_{m,i}}+\frac{r^2{}_c}{15D_{c,i}} \tag{5}$$

The momentum equation can be expressed as follows.

$$\frac{\partial(\varepsilon\rho\vec{v})}{\partial t}+div(\rho\vec{v}\vec{v})=div\left(\bar{\bar{\tau}}\right)-gardP+\rho\vec{g}$$
$$+A\frac{(1-\varepsilon)^2\mu}{\varepsilon_3d^2{}_p}u+B\frac{1-\varepsilon}{\varepsilon^2d_p}\rho u^2 \tag{6}$$

Empirical parameters A and B are often set to 150 and 1.75.

The energy equation can be expressed as follows.

$$\frac{\partial\left(\varepsilon\rho E_g+(1-\varepsilon)\rho_pE_s\right)}{\partial t}+div\left(\vec{v}\left(\rho E_g+P\right)\right)=$$
$$div\left[k_{eff}gradT-\sum_i h_iJ_i+\bar{\bar{\tau}}\vec{v}\right] \tag{7}$$
$$+(1-\varepsilon)\rho_s\sum\nolimits_i-\Delta H_i\frac{\partial q}{\partial t}+h_wA_w(T-T_w)$$

2.2 Performance indicators

The performance indicators of temperature swing adsorption processes are the CO_2 purity, recovery. The calculation method is as below.

$$\text{Purity of } CO_2 = \frac{\int_{t_{startheating}}F_{CO_2}dt}{\sum_i\int_{t_{startheating}}F_idt} \tag{8}$$

$$\text{Recovery of } CO_2 = \frac{\int_{t_{startheating}}F_{CO_2}dt}{\int_{t_{startfeed}}^{t_{startheating}}F_{CO_2}dt} \tag{9}$$

$$F_i=Q_FC_i \tag{10}$$

The energy consumption of temperature swing adsorption process is calculated as below.

$$Q_{chamber}=Q_1+Q_2+Q_3+Q_4+Q_5=$$
$$\frac{\int_{T_{chamber,\max}}^{T_{chamber,\min}}\left(m_sC_{p,s}+m_sq_{CO_2}M_{CO_2}C_{p,CO_2}\right)dT+\int_{T_{wall,\min}}^{T_{wall,\max}}m_wC_wdT_w+\int_{q_{\min}}^{q_{\max}}m_s\Delta Hdq}{q} \tag{11}$$

Coefficient of performance of CO_2 capture (COP_{CO_2}) of temperature swing adsorption process is calculated as below. This indicator which represents the ratio of energy gained and paid during CO_2 capture is an energy efficiency indicator applied to evaluate the energy-efficiency level of carbon capture technologies.

$$COP_{CO_2} = \frac{\text{Gain}}{\text{Payment}} = \frac{\Delta G}{\Delta W} = \frac{(\Delta G_1 + \Delta h_1) + (W_{\min} + \Delta h_2)}{W_{\min} + \Delta h_2} \quad (12)$$

2.3 Validation of the Model

Before investigating the TSA process, the models should validate carefully against experimental data. The characteristics of the fixed bed and system are presented in Table 1. Table 2 gives the parameters used for the Toth model isotherms.

To simplify the calculation, the following assumptions are adopted:

- the gas phase obeys ideal gas law,
- the flow is laminar (Re < 10),
- the porous media is homogenous,
- the physical properties of the adsorbents are constant,
- the Linear Driving Force (LDF) model is used to account for the mass transfer rate during the adsorption process.

Table 1. Chamber geometry and thermal properties of zeolite 13X-APG[14].

Properties	Value
Chamber length, L	0.76 m
Chamber diameter, D_{out}	0.08 m
Internal tube diameter, D_{in}	0.02 m
Chamber wall thickness	0.002 m
Chamber porosity, ε	0.565
Insulation thickness, δ	0.002 m
Adsorbent specific heat capacity, $C_{p,s}$	920 J/kg k
Particle density, ρ_b	1099.5 kg/m^3
Metal material density, ρ_w	502.48 J/kg K
Metal material heat capacity, $C_{p,w}$	8030 J/kg K
CO_2 adsorption heat, ΔH_{CO2}	-26050 J/mol
N_2 adsorption heat, ΔH_{N2}	-13360 J/mol

Table 2. Equilibrium isotherm parameters for zeolite 13X-APG[14].

Gas species	q_m (mmol/g)	K_0 (Pa^{-1})	n	ΔH (J/mol)
CO_2	5.445	5.33e-9	0.5506	-26050
N_2	1.014	2.26e-8	0.4376	-13360

The breakthrough curve is the curve of the ratio of the outlet gas concentration to the inlet gas concentration over time. The breakthrough curves for both the experimental data and the present numerical model results are shown in Fig. 2. It can be seen that the numerical simulation results of both 2D and 3D models are well matched with the experimental results. 3D model of one and three tube are also matched with the experimental results. Therefore, the 3D model can be used in the following simulation work accurately.

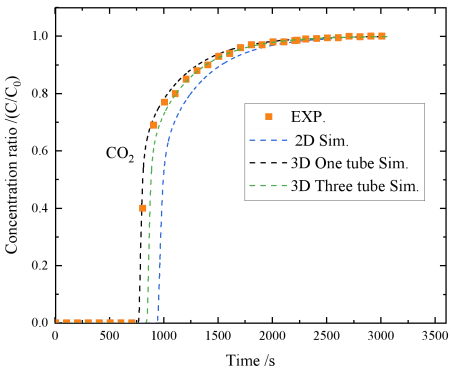

Fig. 2. CO_2 /N_2 concentration ratios

3. RESULTS AND DISCUSSIONS

3.1 TSA cycle

In order to further study the effect of heat exchanger on adsorption, desorption and cooling steps of adsorption chamber, one tube and three tube heat exchanger investigated. Comparison of the two types of heat exchanger are based on the same heat exchange surface area, inlet flow rate, total amount of adsorbent, and operating parameters.

3.2 Boundary conditions

The detailed boundary conditions of the three-step TSA process are shown in Fig. 3. The adsorption process is to feed the adsorption chamber with a mixture gas containing CO_2/N_2 (15% CO_2 , 85% N_2 (mol%)) at 101.3 KPa and 288 K. The inlet condition is “velocity inlet” and the outlet condition is “pressure outlet”. The wall out condition is convection heat transfer with the air at 288 K and the wall in condition is “wall”. During the desorption process, the chamber is heated by internal heat exchanger (wall in) with constant wall temperature boundary conditions (363 K) while the wall in condition is “wall”. At this point, the outlet condition is “the wall” and the inlet condition is “pressure outlet”. Cooling is

required before the next cycle begins. In our case, the adsorption bed reactor is cooled by air. The inlet and outlet boundary conditions of the cooling process are "wall".

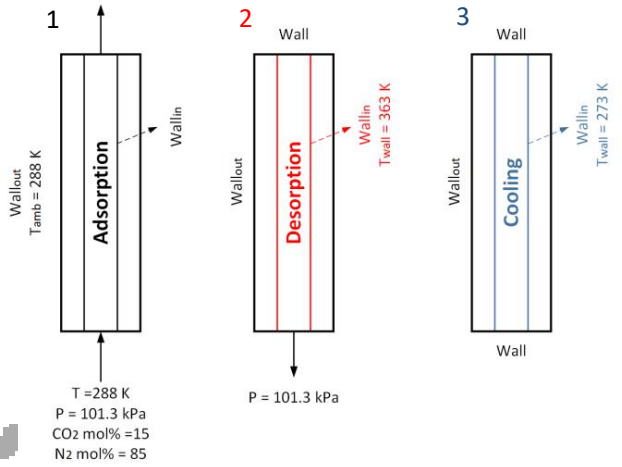

Fig. 3. Boundary conditions for three-step of TSA.

3.3 Inlet speed

Fig. 4 shows the changing trend of the temperature of adsorption chamber in the whole TSA cycle when the inlet speed is 0.1, 0.12, 0.15 and 0.18 m/s. In the adsorption stage, the adsorbent absorbs CO_2 and emits heat, resulting in the rising of the chamber temperature. In the desorption stage, the adsorption chamber is heated by the high temperature steam of the internal heat exchanger, and begins to desorption, leading to the increase of the temperature of the adsorption chamber. During the cooling stage, the adsorption chamber is cooled by the cooling water of the internal heat exchanger, resulting in the chamber temperature dropping to near room temperature. With the increase of the gas inlet speed, the temperature variation trend of the central radial section of the chamber is similar. The higher the inlet speed is, the higher the chamber temperature is. The heating and cooling speed of the chamber also increases with the increase of the inlet speed. With the increase of inlet speed, the adsorption reaction between adsorbent and mixture gas in the adsorption chamber is accelerated, and the convective heat transfer between particles and fluids is strengthened.

Fig. 5 is the radial temperature contour of the adsorption chamber during the three-step TSA process. The inlet speed is 0.15 m/s, which is better for increasing heat transmission. Under the same heat transfer area, the water flow rate in the three-tube heat exchanger will increase, so the heat transfer coefficient will increase accordingly. Therefore, the heat transfer effect of the three-tube heat exchanger is faster and better than that of the one-tube heat exchanger.

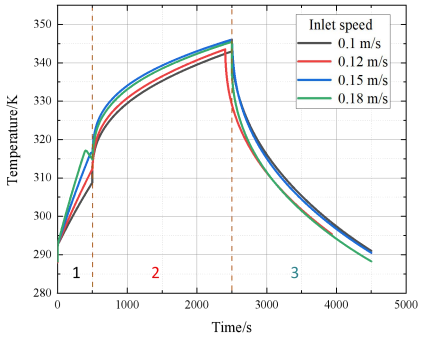

Fig. 4.The influence of inlet speed on the temperature of adsorption chamber

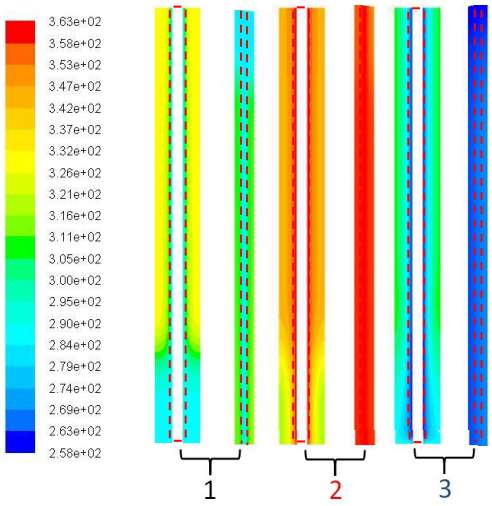

Fig. 5.The radial temperature contour of one tube (Left) and three tube (Right) heat exchanger in chamber under TSA cycle.

Fig. 6 shows the product gas purity and recovery rate after the desorption stage, 500 s is chosen for the desoption time and 0.15 m/s is selected as inlet speed. The purity and recovery of the three-tube heat exchanger in adsorption chamber are larger than that of the one-tube heat exchanger. This is because at the same desorption time, the volume flow rate and concentration at the outlet of the three-tube heat exchanger are higher than that of the one-tube heat exchanger, which leads to the better separation performance of the three-tube heat exchanger. Fig. 7 shows the specific energy consumption and COP_{CO_2} varies with inlet speed. Under the same other conditions, the energy consumption of each part in the adsorption chamber decrease from 6316.76 to 6278.19 kJ/kg_{CO2} (one tube) and from 5868.11 to 5366.82

kJ/kg_{CO2} (three tube) when the inlet speed is changed only. The specific energy consumption of three-tube heat exchanger in adsorption chamber is lower than one-tube heat exchanger. At the same time, as the inlet speed increases, the COP_{CO_2} increase from 2.01 to 2.02 (one tube) and from 2.08 to 2.21 (three tube). The COP_{CO_2} of three-tube heat exchanger in adsorption chamber is higher than one-tube heat exchanger. Therefore, proper improvement of inlet speed and the use of three-tube heat exchanger in adsorption chamber can effectively improve the energy efficiency performance of TSA cycle and enhance heat and mass transfer effect.

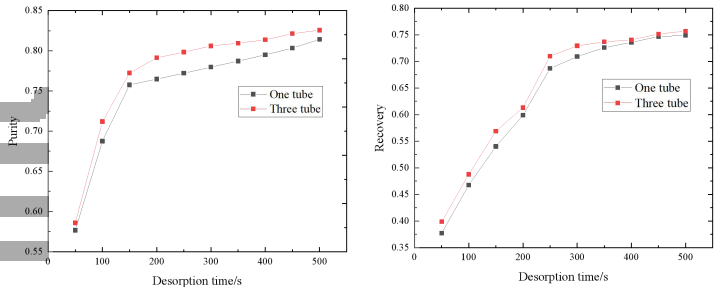

(a)Purity (b) Recovery

Fig. 6. CO_2 Purity (a) and Recovery rate (b) varies with desorption time.

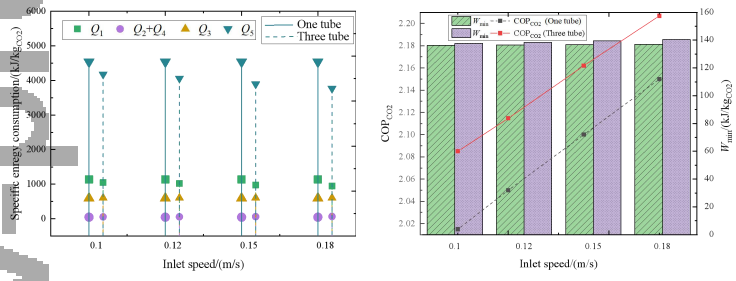

(a) Specific energy consumption (b) COP_{CO2}

Fig. 7. Specific energy consumption (a) and COP_{CO_2} (b) varies with inlet speed.

3.4 Porosity

Fig. 8 shows the changing trend of the temperature of adsorption chamber in the whole TSA cycle when the porosity is 0.565, 0.676, 0.751 and 0.852. With the increase of the porosity, the temperature variation trend of the central radial section of the chamber is similar. The higher the porosity is, the faster the chamber is heated or cooled. This is because the thermal conductivity of the adsorbent is 0.2 W/m K, less than the thermal conductivity of the water is 0.55 W/m K, the porosity increases, and the convective heat transfer between the particles and the fluid is strengthened.

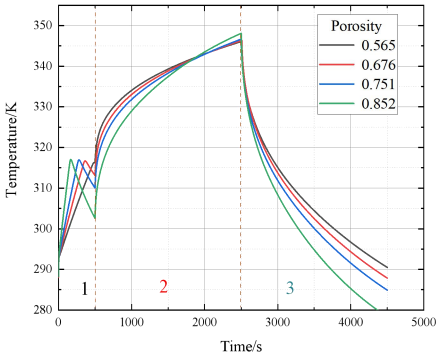

Fig. 8.The influence of porosity on the temperature of adsorption chamber

Fig. 9 shows the CO_2 purity and recovery rate after the desorption stage, 500 s is chosen for the desoption time and 0.676 is selected as porosity. The purity and recovery of the three-tube heat exchanger in adsorption chamber are larger than that of the one-tube heat exchanger. As the temperature difference between the adsorption chamber and the heating fluid decreases, the rate of chamber heating slows down.The temperature difference of the three tube is smaller, so the separation performance is stronger. Fig. 10 shows the specific energy consumption and COP_{CO_2} varies with porosity. At the same other conditions , as the porosity increases, the energy consumption of each part in the adsorption chamber decrease from 6316.76 to 5820.82 kJ/kg_{CO2} (one tube) and from 5521.87 to 5225.36 kJ/kg_{CO2} (three tube), the COP_{CO_2} increase from 2.01 to 2.04 (one tube) and from 2.16 to 2.19 (three tube). Therefore, appropriately increasing porosity can improve TSA process energy efficiency.

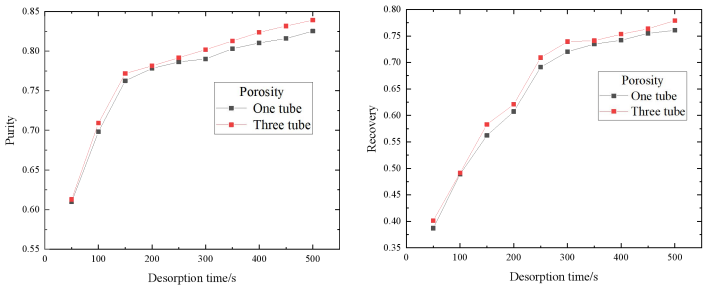

(a)Purity (b) Recovery

Fig. 9. CO_2 Purity (a) and Recovery rate (b) varies with desorption time.

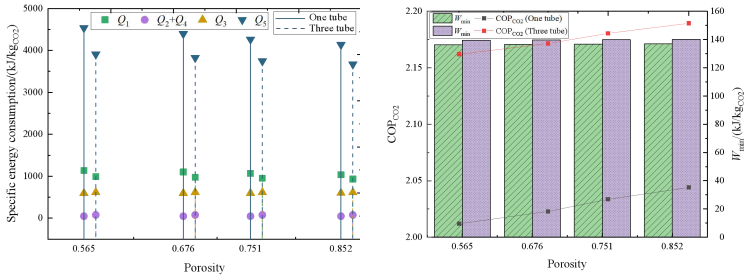

(a) Specific energy consumption (b) COP_{CO2}

Fig. 10. Specific energy consumption (a) and COP_{CO_2} (b) varies with porosity.

4. CONCLUSIONS

This paper focus on the the energy efficiency performance of the adsorption chamber that contains the inner heat exchanger based on TSA process. According to numerical simulations and analysis, the number of heat exchanger, inlet speed and porosity are all related to purity, recovery rate, specific energy consumption and COP_{CO_2}.

(1) Under the same operating conditions, the CO_2 purity, recovery rate and COP_{CO_2} of the three-tube heat exchanger in adsorption chamber are higher than that of the one-tube heat exchanger, with lower energy consumption of three-tube heat exchanger. Therefore, the three-tube heat exchanger in the adsorption chamber is helpful to enhance heat transfer and mass transfer and improve the energy efficiency of TSA process.

(2) The temperature distribution of the adsorption chamber is greatly influenced by the inlet speed and porosity. By increasing inlet speed or porosity, the CO_2 purity, recovery rate and COP_{CO_2} can be improved and energy consumption can be reduced.

(3) This paper will further study the effects of heat exchanger types (such as finned tube), adsorption and desorption temperature, length-diameter ratio and other factors on the energy efficiency performance of TSA cycle. And then do some theoretical guidance for engineering design.

ACKNOWLEDGEMENT

The authors are grateful for the support provided by The National Key Research and Development Program of China under Grant No. 2017YFE0125100, General Program of National Natural Science Foundation of China under Grant No. 51876134, and Research Plan of Science and Technology of Tianjin City under Grant No.18YDYGHZ00090.

REFERENCE

[1] During the 75th Session of the United Nations General Assembly, China pledged to achieve carbon neutrality by 2060 [EB/OL]. https://www.zhihu.com/.

[2] Ben-Mansour R, Qasem NAA. An efficient temperature swing adsorption (TSA) process for separating CO_2 from CO_2 /N_2 mixture using Mg-MOF-74. Energ Convers Manage 2018; 156: 10-24.

[3] Drage TC, Snape CE, Stevens LA. Materials challenges for the development of solid sorbents for post-combustion carbon capture. J Mater Chem 2012; 22.

[4] Harlick PJ, Handan Tezel F. An experimental adsorbent screening study for CO_2 removal from N2. Microporous Mesoporous Mater 2004; 76: 71–79.

[5] Samanta A, Zhao A, Shimizu GKH. Post-combustion CO_2 capture using solid sorbents: a review. Ind Eng Chem Res 2012; 51: 1438–1463.

[6] Lively RP, Chance RR, Koros WJ. Enabling low-Cost CO_2 capture via heat integration. Ind Eng Chem Res 2010; 49: 7550–7562.

[7] Bonjour J, Clausse M, Meunier F. A TSA process with indirect heating and cooling: parametric analysis and scaling-up to practical sizes. Chem Eng Process 2005; 44: 969-977.

[8] Baudu M, Le Cloirec P, Martin G. Thermal regeneration by Joule effect of activated carbon used for air treatment. Environ Technol 1992; 13: 423-435.

[9] Yu FD, Luo LA, Grévillot G. Electrothermal desorption using Joule effect on an activated carbon monolith. J Environ Eng 2004; 130: 242-248.

[10] Mezey EJ, Dinovo ST. Adsorbent regeneration and gas separation utilizing microwave heating, US Patent 4322394 (1980).

[11] Bonnissel M, Luo L, Tondeur D. Fast thermal swing adsorption using thermoelectric devices and new adsorbent, in: Proceedings of the Sixth Conference on Fundamentals of Adsorption (FOA6), 1998, 1065-1070.

[12] Lian YH, Deng S, Li SJ. Numerical analysis on CO_2 capture process of temperature swing adsorption (TSA): Optimization of reactor geometry. Int J Greenh Gas Con 2019; 85: 187-198.

[13] Farooq S, Ruthven DM. Heat effects in adsorption column dynamics: Experimental validation of the one-dimensional model. Ind Eng Chem Res 1990; 29.

[14] Liu BW, Lian YH, Li SJ. Experimental investigation on separation and energy-efficiency performance of temperature swing adsorption system for CO_2 capture. Sep Purif Technol 2019; 227, 115670.